Correlation between the atomic structures and the misorientation angles of [0001]-tilt grain boundaries at triple junctions in ZnO thin films grown on Si substrates

J. W. Shin and J. Y. Lee
*Department of Materials Science and Engineering, Korea Advanced Institute of Science and Technology,
Daejeon 305-701, Korea*

Y. S. No and T. W. Kim[a)]
*Advanced Semiconductor Research Center, Division of Electronics and Computer Engineering,
Hanyang University, 17 Haengdang-dong, Seongdong-gu, Seoul 133-791, Korea*

W. K. Choi
Thin Film Material Research Center, Korea Institute of Science and Technology, Seoul 136-701, Korea

The correlation between the atomic structures and the misorientation angles of [0001]-tilt grain boundaries at triple junctions in ZnO thin films grown on Si substrates was investigated by using high-resolution transmission electron microscopy (HRTEM) measurements. The HRTEM images showed three symmetric grain boundaries and one asymmetric grain boundary around the triple junction in the ZnO film. The correlation between the atomic structures and the misorientation angles of the grain boundaries at triple junctions in ZnO films is described on the basis of the HRTEM results. © *2006 American Institute of Physics*. [DOI: 10.1063/1.2338792]

Potential applications of optoelectronic devices operating in the blue region of the spectrum utilizing II-VI semiconductor epitaxial films with large energy gaps have driven extensive efforts to grow ZnO thin films on various substrates.[1–3] ZnO thin films have become particularly attractive because of the interest in investigating the fundamental physical properties of the films and their potential applications in many promising devices.[4,5] Since ZnO thin films are wide band-gap semiconductors with unique physical properties of large exciton binding energies and excellent chemical stabilities,[4,5] they are particularly interesting due to their potential applications in optoelectronic devices, such as light-emitting diodes,[6] laser diodes,[7] and solar cells.[8] In particular, ultraviolet lasers fabricated utilizing ZnO thin films operating at room temperature have emerged as potential candidates for applications in next-generation promising optoelectronic devices.[9–12] Since the optical properties of ZnO thin films grown on Si substrates are significantly affected by the microstructural properties related to the grain boundaries of the films, studies concerning the atomic structures of the grain boundaries in ZnO thin films are very important for improving the efficiencies of optoelectronic devices. Many theoretical works have extensively addressed the microstructural properties of [0001]-tilt boundaries in materials with a wurtzite structure.[13–21] Even though some experimental works exist on the atomic structure of [0001]-tilt grain boundaries of materials with a wurtzite structure, such as ZnO[22,23] and GaN,[24] almost all works have been confined to particular grain boundaries. However, studies concerning the correlation between the atomic structures and the misorientation angles of [0001]-tilt grain boundaries at a triple junction of materials with a wurtzite structure have not yet been performed. Furthermore, investigations of the grain bound-

aries at a triple junction in the ZnO thin films are very important for understanding the deterioration of optoelectronic devices fabricated utilizing the films.

This letter reports systematic investigations of the correlation between the atomic structures and the misorientation angles of [0001]-tilt grain boundaries at triple junctions in ZnO thin films grown on *p*-Si substrates by using the radio-frequency magnetron sputtering method. Transmission electron microscopy (TEM) measurements were performed to investigate the microstructural properties of the as-grown and the annealed ZnO thin films. The correlation between the atomic structures and the misorientation angles of the [0001]-tilt ZnO grain boundaries at triple junctions is described on the basis of the high-resolution TEM (HRTEM) results.

Polycrystalline stoichiometric ZnO with a purity of 99.999% was used as a source target material and was pre-cleaned by repeated sublimation. The carrier concentration of the B-doped *p*-Si substrates with (100) orientation used in this experiment was 1×10^{15} cm^{-3}. The substrates were degreased in trichloroethylene (TCE), rinsed in de-ionized water, etched in a mixture of HF and H_2O (1:1) at room temperature for 5 min, and rinsed in TCE again. After the Si wafers had been cleaned chemically, they were mounted onto a susceptor in the growth chamber. After the chamber had been evacuated to 8×10^{-7} Torr, the deposition was done at a substrate temperature of 600 C. An Ar gas with a purity of 99.999% was used as the sputtering gas. Prior to ZnO growth, the surface of the ZnO target was polished by Ar$^+$ sputtering. The ZnO deposition was done at a system pressure of 0.021 Torr and a radio-frequency power (radio frequency=13.26 MHz) of 100 W. The flow-rate ratio of Ar to O_2 was 2, and the growth rate was approximately 1.17 nm/min.

The TEM measurements were performed using a JEM-ARM1300S transmission electron microscope operating at

---

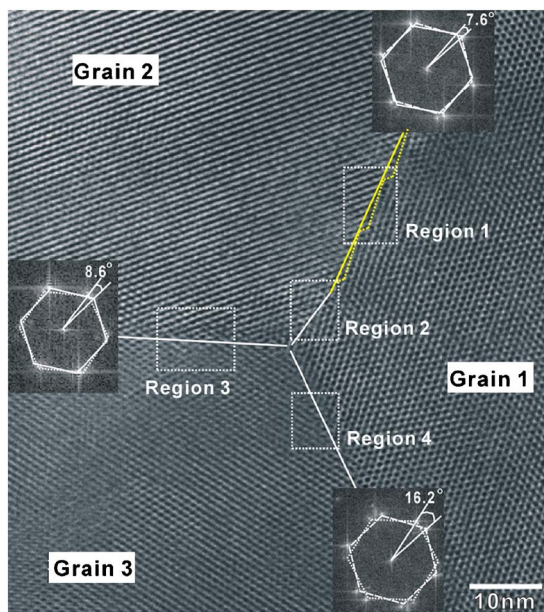[a)]Author to whom correspondence should be addressed; electronic mail: twk@hanyang.ac.kr

FIG. 1. HRTEM image around a triple junction in the annealed ZnO films grown on *p*-Si (100) substrates.

FIG. 3. (a) Magnification of region 2 in the HRTEM image shown in Fig. 1 and (b) corresponding schematic diagram of the atomic structure: the symmetric tilt grain boundary with a rotation angle of 8.6° and the symmetric tilt grain boundary in the coincident site lattice notation of near $\Sigma 37$ ($34\bar{7}0$). Burgers circuits are drawn along $\{10\bar{1}0\}$ planes.

1.25 MeV. The samples for the plan-view TEM measurements were prepared by cutting and polishing with diamond paper to a thickness of approximately 30 μm and then argon-ion milling at liquid-nitrogen temperature to electron transparency.

Figure 1 shows a HRTEM image around a triple junction in the annealed ZnO thin films grown on *p*-Si (100) substrates. The rotation angles of the [0001]-tilt boundaries, estimated from fast Fourier transforms of the HRTEM images, are 7.6°, 8.6°, and 16.2°. The [0001]-tilt grain boundaries in the HRTEM image appear at an angle below 20°, which corresponds to the low angle grain boundary. Since the dislocation spacing at an angle above 20° is so small that the dislocation cores overlap, an identification of the each dislocation is not possible. One asymmetric grain boundary, which is the periodic $\{10\bar{1}0\}$ facet structure, is shown in region 1 of Fig. 1 and is 7 to 1, indicative of the microstructural grain boundary ($17\bar{8}0$) of grain 1. However, since the asymmetric tilt grain boundary is not suitable for the existence of the highly distorted atomic structure, an unstable plane is generated. Even though grains 1 and 2 have asymmetric grain boundaries, they change into a symmetric grain boundary ($45\bar{9}0$) around a triple junction, as shown in Fig. 1. Three symmetric grain boundaries with fully accommodated
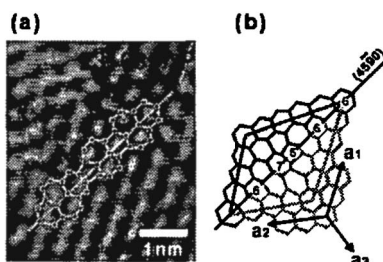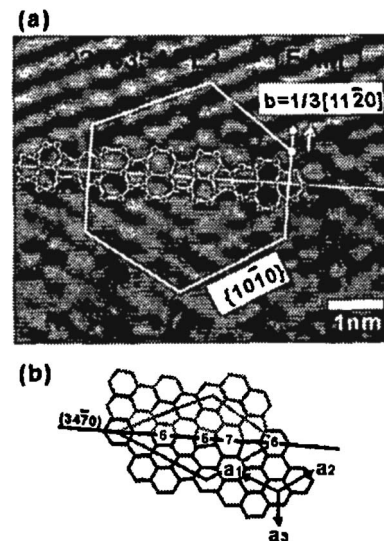
misorientations, which are denoted by regions 2, 3, and 4, appear around the triple junction due to the stabilization of the energy, resulting from the relaxation of the misfit between grains.

Magnifications of regions 2, 3, and 4 in the HRTEM images and corresponding schematic diagrams of the atomic structures are shown in Figs. 2, 3, and 4, respectively. The coincident site lattice notations with rotation angles of 7.6°, 8.6°, and 16.2° are approximately $\Sigma 61$ ($45\bar{9}0$), $\Sigma 37$ ($34\bar{7}0$), and $\Sigma 49$ ($35\bar{8}0$), respectively. These symmetrical tilt grain boundaries (STGBs) are formed by a pair of five and seven coordinated channels. The Burgers circuits, which are described on the basis of the bright spots representing the primitive cell edges, indicate that five and seven coordinated channels are obtained from the edge dislocation with a Burgers vector of $1/3\langle 11\bar{2}0\rangle$, as shown in Fig. 3. The boundary consisting of the dislocation array is typically referred to as a low angle boundary. The misorientation might be fully accommodated by dislocations at STGBs with a low angle. The symmetric period formed on the basis of the sequences of 66657, 6657, and 65757 coordinated channels for 7.6°, 8.6°,

FIG. 2. (a) Magnification of region 1 in the HRTEM image shown in Fig. 1 and (b) corresponding schematic diagram of the atomic structure: the symmetric tilt grain boundary with a rotation angle of 7.6° and the symmetric tilt grain boundary in the coincident site lattice notation of near $\Sigma 61$ ($45\bar{9}0$).
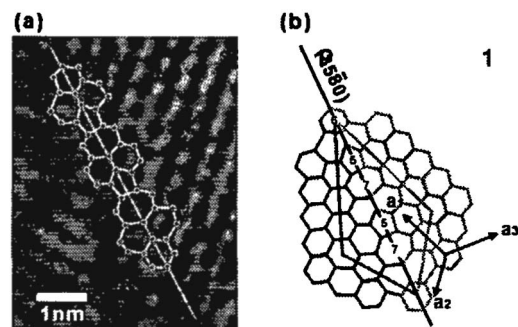

FIG. 4. (a) Magnification of region 3 in the HRTEM image shown in Fig. 1 and (b) corresponding schematic diagram of the atomic structure: the symmetric tilt grain boundary with a rotation angle of 16.2° and the symmetric tilt grain boundary in the coincident site lattice notation of near $\Sigma 49$ ($35\bar{8}0$).
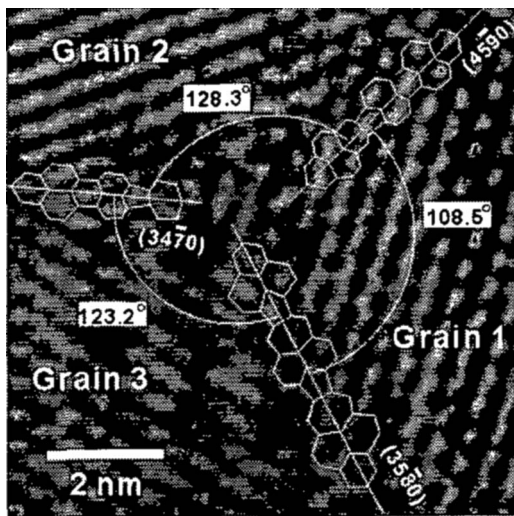
FIG. 5. HRTEM image at the triple junction. Reference structures of the symmetric grain boundaries are $\Sigma 61$, $\Sigma 37$, and $\Sigma 49$.

and 16.2° tilted symmetric grain boundaries, respectively, indicates that the grain boundary energy γ is approximately proportional to the tilt angle of θ because the energy of the grain boundary with a low angle is related to the total energy of the dislocation per unit length of the grain boundary.[25] This result is in reasonable agreement with the low-energy configuration of [0001]-tilt boundary in GaN (Ref. 13) in spite of a difference in the ionicity and the covalency between ZnO and GaN materials. The atomic structure of the [0001]-tilt boundary in the wurzite materials is mainly determined by geometric and symmetric constrains.[22]

The experimental angles between grains 1 and 2 (α_1), grains 1 and 3 (α_2), and grains 2 and 3 (α_3), as determined from the HRTEM image shown in Fig. 5, are 108.5°, 128.3°, and 123.2°, respectively. The reference structures formed on the basis of the sequences of 66657, 6657, and 65757 are also shown in Fig. 5. Since the energy of the grain boundary is related to the total energy of the dislocation per unit length,[25] the relative values of the grain boundary energies are $\gamma_{13} > \gamma_{23} > \gamma_{12}$, where γ_{13}, γ_{23}, and γ_{12} are the boundary energies between grains 1 and 3, grains 2 and 3, and grains 1 and 2, respectively. Therefore, the angle between the grain boundaries should be $\alpha_2 > \alpha_1 > \alpha_3$, resulting from the relationships between the boundary energies and the angles of the grain boundaries.[25] However, the experimental angles of α_1, α_2, and α_3 are not consistent with theoretical values. The differences between the angles obtained from the HRTEM image and the theoretical angles originate from the preferential formation of the STGBs with the most stable state. Therefore, the actual grain boundary angles at a triple junction in the stable ZnO film are constructed by the correlation between the STGBs, which are affected by the tilted angles, due to the relaxation of the stress resulting from the formation of the dislocations. Since the misorientation between grains can be fully accommodated due to the dislocation in the STGB, the grain boundary tends to change from an asymmetric tilt grain boundary to a STGB during the thermal annealing process.

In summary, four types of grain boundaries at a triple junction were observed and consisted of three symmetric grain boundaries of $(34\bar{7}0)$, $(35\bar{8}0)$, and $(45\bar{9}0)$ grain boundaries and one periodic $\{10\bar{1}0\}$ facet structure of a $(17\bar{8}0)$ microstructural grain boundary. The STGBs with stable grain structures were preferentially formed by accommodation of the misorientation due to the dislocations during annealing. A possible correlation between atomic structures and the misorientation angles of the grain boundaries at a triple junction in a ZnO film is describe on the basis of the HRTEM results.

[1] D. M. Bagnall, Y. F. Chen, Z. Zhu, T. Yao, M. Y. Shen, and T. Goto, Appl. Phys. Lett. **73**, 1038 (1998).
[2] J. H. Choi, H. Tabata, and T. Kawai, J. Cryst. Growth **226**, 493 (2001).
[3] A. Nahhas, H. K. Kim, and J. Blachere, Appl. Phys. Lett. **78**, 1511 (2001).
[4] T. Aoki, Y. Hatanaka, and D. C. Look, Appl. Phys. Lett. **76**, 3257 (2000).
[5] R. F. Service, Science **276**, 895 (1997).
[6] Y. Liu, C. R. Gorla, S. Liang, N. Emanetoglu, Y. Lu, H. Shen, and M. Wraback, J. Electron. Mater. **29**, 69 (2000).
[7] H. Kim, C. M. Gilmore, J. S. Horwitz, A. Piqué, H. Murata, G. P. Kushto, R. Schlaf, Z. H. Kafafi, and D. B. Chrisey, Appl. Phys. Lett. **76**, 259 (2000).
[8] U. Rau and M. Schmidt, Thin Solid Films **387**, 141 (2001).
[9] Z. K. Tang, G. K. L. Wong, P. Yu, M. Kawasaki, A. Ohtomo, H. Koinuma, and Y. Segawa, Appl. Phys. Lett. **72**, 3270 (1998).
[10] Y. Chen, D. M. Bagnall, Z. Zhu, T. Sekiuchk, K. Park, K. Hiraga, T. Yao, S. Koyama, M. Y. Shen, and T. Goto, J. Cryst. Growth **181**, 165 (1997).
[11] D. M. Bagnall, Y. F. Chen, Z. Zhu, T. Yao, S. Koyama, M. Y. Shen, and T. Goto, Appl. Phys. Lett. **70**, 2230 (1997).
[12] Y. Segawa, A. Ohtomo, M. Kawasaki, H. Koinuma, Z. K. Tang, P. Yu, and G. K. L. Wong, Phys. Status Solidi B **202**, 669 (1997).
[13] J. Chen, P. Ruterana, and G. Nouet, Phys. Rev. B **67**, 205210 (2003).
[14] A. Bere and A. Serra, Phys. Rev. B **66**, 085330 (2002).
[15] J. D. Rittner and D. N. Seidman, Phys. Rev. B **54**, 6999 (1996).
[16] M. Kohyama, Modell. Simul. Mater. Sci. Eng. **10**, R31 (2002).
[17] S. D. Mo, W. Y. Ching, M. F. Chisholm, and G. Duscher, Phys. Rev. B **60**, 2416 (1999).
[18] S. Fabris and C. Elsässer, Phys. Rev. B **64**, 245117 (2001).
[19] F. Oba, I. Tanaka, S. R. Nishitani, H. Adachi, B. Slater, and D. H. Gay, Philos. Mag. A **80**, 1567 (2000).
[20] F. Oba, S. R. Nishitani, H. Adachi, I. Tanaka, M. Kohyama, and S. Tanaka, Phys. Rev. B **63**, 045410 (2001).
[21] J. M. Carlsson, B. Hellsing, H. S. Domingos, and P. D. Bristowe, J. Phys.: Condens. Matter **13**, 9937 (2001).
[22] F. Oba, H. Ohta, Y. Sato, H. Hosono, T. Yamamoto, and Y. Ikuhara, Phys. Rev. B **70**, 125415 (2004).
[23] Y. Sato, T. Mizoguchi, F. Oba, M. Yodogawa, T. Yamamoto, and Y. Ikuhara, J. Mater. Sci. **40**, 3059 (2005).
[24] V. Potin, P. Ruterana, G. Nouet, R. C. Pond, and H. Morkoç, Phys. Rev. B **61**, 5587 (2000).
[25] D. A. Porter and K. E. Easterling, *Phase Transformations in Metals and Alloys* (Nelson Thornes, Cheltenham, 1991), Vol. 1, p. 127–133.